The effects of installation disturbance on interpretation of in situ tests in clay

A.J. WHITTLE and C.P. AUBENY, Massachusetts Institute of Technology

In his 1984 Rankine lecture, Professor Wroth emphasized the need for a theoretical basis in order to develop meaningful correlations between engineering properties of soils and in situ test measurements. This paper describes an analytical framework for predicting in situ test measurements using: the Strain Path Method, to simulate soil disturbances caused by device installation; and a generalized effective stress soil model (MIT-E3), which is capable of modelling the anisotropic stress–strain response of soft clays. Predictions of piezocone penetration are evaluated through direct comparison with field measurements in Boston Blue clay. The analyses show that undrained shear strength can be estimated reliably from the measured cone resistance or tip pore pressures. Strain path analyses for flat plate penetrometers show the similarity between contact pressures measured by the dilatometer and lateral stresses around the shaft of an axisymmetric penetrometer. Installation disturbance also affects the interpretation of undrained shear strength from pressuremeter expansion tests. For displacement pressuremeters, the installation conditions lead to an underestimation of the derived shear strength; while simplified analyses of self-boring explain, in part, the overprediction of undrained shear strength frequently reported from self-boring pressuremeter tests.

Introduction

The mechanical installation of in situ test devices in the ground inevitably causes disturbance of the surrounding soil. For devices such as the piezocone, measurements of tip resistance and excess pore pressures during penetration are manifestations of stress changes induced in the soil by the installation process. Qualitatively similar disturbances can be expected from other 'displacement' penetrometers including earth pressure cells, field vanes, the Marchetti dilatometer, Iowa stepped blade, push-in pressuremeter, etc. In contrast, the design of the self-boring pressuremeter (SBPM; e.g. Wroth and Hughes (1972)) attempts to minimize disturbance by removing soil in order to accommodate the volume of the device.

This paper describes numerical analyses which quantify installation

stresses and pore pressures for in situ tests in clays, and summarizes results that illustrate how soil disturbance affects the subsequent interpretation of engineering properties from these measurements. The study uses the Strain Path Method (SPM; Baligh (1985, 1986a, b)) to simulate the mechanics of quasi-static, undrained, deep penetration in clays. Changes in effective stresses and soil properties throughout the tests are computed using the Modified Cam Clay (MCC; Roscoe and Burland (1968)) and MIT-E3 (Whittle, 1990, 1992) effective stress soil models.

The presentation focuses on site-specific predictions of piezocone, dilatometer and pressuremeter measurements in Boston Blue Clay (BBC). Extensive laboratory test data for this material enable the predictive capabilities of the soil models to be evaluated thoroughly at the element level. These comparisons highlight the importance of anisotropic stress–strain properties for K_0-consolidated clays.

The main aim of the analyses is to predict the in situ measurements based on a known set of soil properties. Direct comparisons with field data can then be used to evaluate the reliability of the analytical methods. The analyses also guide the interpretation of in situ tests by establishing the relative merits of correlations between measurements and engineering properties of the soil. Results presented in this paper compare correlations of undrained shear strength with

(*a*) tip resistance and pore pressure measurements from piezocone tests
(*b*) dilatometer contact pressures
(*c*) expansion and contraction curves for displacement and self-boring pressuremeter tests.

Strain path analyses of in situ tests

The analysis of deep penetration in soils represents a highly complex problem due to:

(*a*) high gradients of the field variables around the penetrometer
(*b*) large deformations and strains which develop in the soil
(*c*) the complexity of the constitutive behaviour of soils, including non-linear, inelastic, anisotropic, and frictional response
(*d*) non-linear penetrometer–soil interface characteristics.

The Strain Path Method (SPM; Baligh (1985)) assumes that, due to the severe kinematic constraints in deep penetration, deformations and strains are essentially independent of the shearing resistance of the soil and can be estimated with reasonable accuracy based only on kinematic considerations and boundary conditions. For piezocone tests performed in low permeability clays, existing strain path analyses assume that there is no migration of pore water during penetration and hence, the soil is sheared in an undrained mode. The strain paths of individual soil elements are estimated using approximate velocity fields obtained from potential theory (i.e. treating the soil as an incompressible, inviscid and irrotational fluid).

The SPM analyses can simulate two or three-dimensional deformations of the soil elements and hence, provide a more realistic framework for describing the mechanics of deep penetration than one-dimensional (cylindrical or spherical) cavity expansion methods. On the other hand, the assumptions of strain-controlled behaviour greatly simplify the problem of deep penetration and avoid the computational complexity of comprehensive, non-linear finite element analyses.

Figure 1(a) shows contours of the octahedral shear strain, E (the second invariant of the deviatoric strain tensor) around an axisymmetric 'simple pile' penetrometer (Baligh, 1985, 1986). For this geometry, the soil deformations are proportional to the radius of the penetrometer, R, and strains can be expressed analytically at all locations. Baligh (1986a) shows that soil elements experience complex strain histories involving reversals of individual shear strain components which cannot be duplicated using existing laboratory equipment. For isotropic soils (modelled as linearly elastic–perfectly plastic materials), the zone of disturbance around the penetrometer can be equated with the contour, $E = E_y$, where E_y is the yield strain of the soil. Baligh (1986a) reports $E_y \approx 0.4\%$ for normally consolidated Boston Blue clay and hence, soil disturbance extends to a radial distance $r/R \approx 10$.

Whittle et al. (1991) have shown that strain path solutions for the simple pile geometry provide a close approximation for the stresses and pore pressures predicted around a standard 60° cone penetrometer. Thus, the simple pile geometry is used throughout this study to estimate installation disturbance for piezocone and 'cone–pressuremeter' devices.

Figure 1(b) presents similar strain paths solutions for a 'simple plate' penetrometer (Whittle et al., 1991), characterized by a length-to-width aspect ratio, $B/w = 20$. The simple plate geometry simulates the mechanics of penetration for flat plate-shaped penetrometers such as the Marchetti dilatometer ($B/w = 6.8$), earth pressure cells ($B/w = 15$–25), and the field vane ($B/w = 32.5$ for the standard Geonor field vane). The equivalent radius R_{eq} ($\approx\sqrt{4Bw/\pi}$) controls the lateral extent of disturbance caused by plate installation (i.e. at locations far from the penetrometer, soil strains and displacements depend only on the volume of soil displaced); while the aspect ratio B/w, affects the strain history of soil elements close to the penetrometer.

Strain path solutions have also been presented for open-ended piles and thin-walled sampling tubes (Baligh et al., 1987) which penetrate the soil in an 'unplugged mode'. Figure 1(c) illustrates the octahedral shear

strains for a simple tube penetrometer with a diameter-to-wall thickness ratio, $B/t = 12$, which simulates approximately the disturbance caused by a push-in pressuremeter device (PIPM). The analyses indicate that the region of high shear strains ($E>10\%$) occurs within a thin annulus around the tube (with dimensions similar to the wall thickness), while the disturbance of the soil is controlled by the volume of soil displaced (for a thin walled tube, $R_{eq} \approx \sqrt{Bt}$).

In contrast to displacement penetrometers, the installation of the self-boring pressuremeter (SBPM) extracts soil from the system in order to accommodate the volume of the device. In practice, this is accomplished by grinding or jetting the soil into a slurry as it enters the cutting shoe, and then flushing it to the surface. A comprehensive analysis of this process is currently not conceivable. Figure 1(d) illustrates an approximate analysis which models the influence of soil extraction on

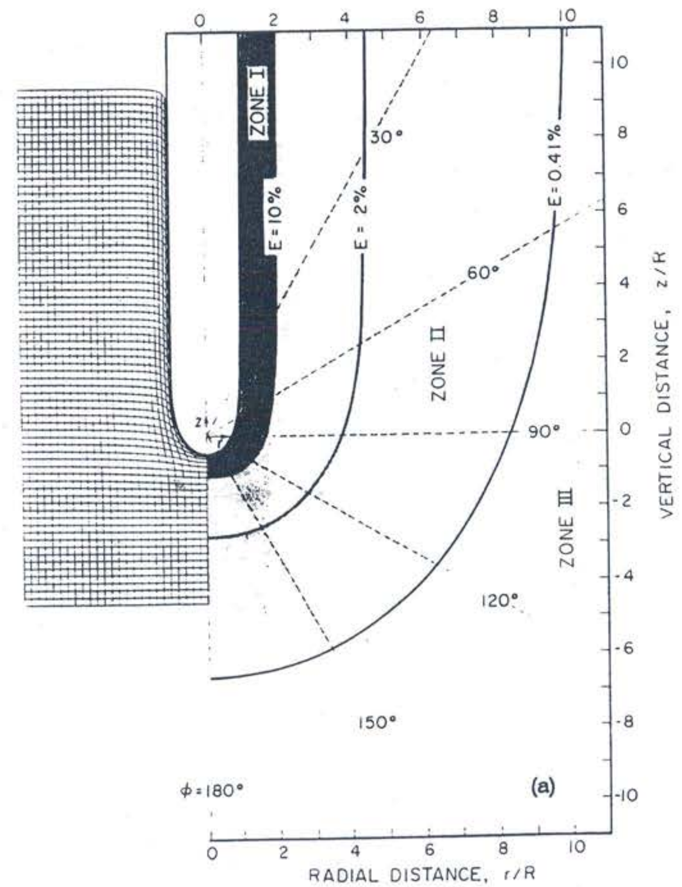

Fig. 1. Shear strains for in situ tests: (a) simple pile

Fig. 1 (below and facing page). Shear strains for in situ tests: (b) simple plate, $B/w = 20$, (c) push-in pressuremeter, (d) ideal self-boring pressuremeter

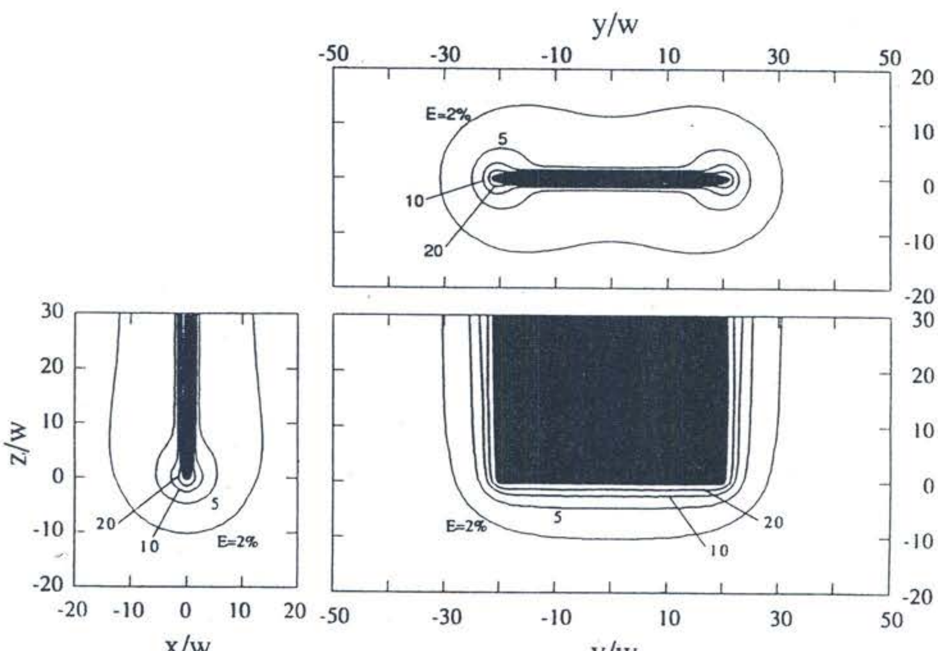

(b)

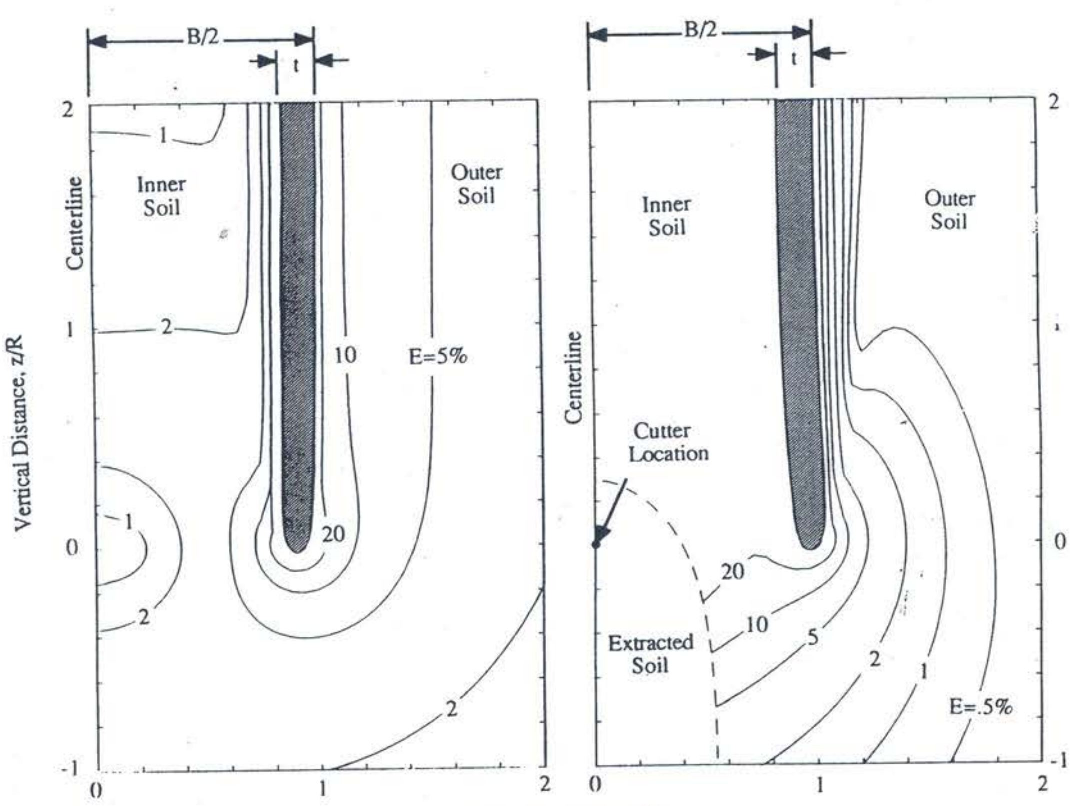

(c) (d)

strains in the outer soil. The analysis simulates soil extraction using a point sink centrally located at the tip of the cutting shoe. For steady penetration, the rate of soil extraction can be conveniently expressed by the ratio, $f = V^-/V^+$, where V^+ and V^- are the strengths of the source (which generates the tube geometry) and sink, respectively. Ideal self-boring penetration occurs for $f = 1$, when the rate of soil extraction exactly balances the displacement due to the pressuremeter tube. The analyses presented in this paper consider a range of f values, $0 \leq f \leq 1$ which correspond to the transition between the PIPM and ideal SBPM tests. Figure 1(*d*) shows that, although self-boring greatly reduces the lateral extent of disturbances in the soil, significant shear strains do develop ahead of the cutting shoe.

One important issue not addressed directly in the strain path analyses is the partial drainage of pore pressures which can occur during penetration. Elghaib (1989) has developed a simplified analysis of partial drainage for piezocone tests in clays and silts. For a piezocone with radius, $R = 1.78$ cm, penetrating at a steady rate, $U = 2$ cm/s, these linear analyses show that partial drainage is not significant when the consolidation coefficient, $c \leq 0.1$ cm²/s. According to these calculations, piezocone penetration in Boston Blue clay ($0.3 \times 10^{-3} \leq c_v \leq 3.0 \times 10^{-3}$ cm²/s) is effectively undrained. The equivalent radius is the primary factor affecting partial drainage for other displacement devices which are installed at the same nominal penetration rate. For devices with R_{eq} similar to the piezocone, the penetration process is effectively undrained. Rates of penetration by self-boring in Boston Blue Clay range from $0.03 \leq U \leq 0.2$ cm/s. In this case, partial drainage may affect the subsequent measurements during the pressuremeter test.

In the current application of the Strain Path Method, effective stresses, σ'_{ij}, are computed directly from the strain paths of individual soil elements using an effective stress–strain soil model (see next section). This approach can be contrasted with previous total stress analyses (Levadoux and Baligh, 1980; Baligh, 1986a; Teh and Houlsby, 1991) which compute shear stresses through a deviatoric stress–strain model, and introduce a separate model for shear induced pore pressures. The main advantage of the effective stress analysis is that the same soil model can be used to study stress changes after installation and throughout subsequent test procedures.

Equilibrium conditions control the penetration excess pore pressures in the Strain Path Method. However, due to the approximations used in the analysis, the equilibrium equations are not satisfied uniquely. Throughout this work, excess pore pressures are obtained by computing the divergence of the equilibrium equations and solving the resulting Poisson type equation using finite element methods (Aubeny, 1992).

Evaluation of soil models for Boston Blue Clay

Although simple models of soil behaviour provide useful physical insights into the underlying mechanics of undrained deep penetration in clays (e.g. Baligh, 1986a; Teh and Houlsby, 1991), more comprehensive constitutive equations are necessary in order to achieve reliable predictions of stress and pore pressure fields for real soils. The analyses presented in this paper use two particular effective stress models to describe clay behaviour:

(1) Modified Cam Clay (MCC; Roscoe and Burland (1968)) is the most widely used effective stress model in geotechnical analysis. The model formulation uses the incremental theory of rate independent elasto-plasticity and is characterized by an isotropic yield function, associated plastic flow and density hardening. The version of the model used in this study uses a von Mises generalization of the yield surface.
(2) MIT-E3 (Whittle, 1990, 1992) is a significantly more complex elasto-plastic model which describes many aspects of the rate-independent behaviour of K_0-consolidated clays, which exhibit normalized behaviour, including:
- (*a*) small-strain non-linearity
- (*b*) anisotropic stress–strain–strength
- (*c*) hysteretic and inelastic behaviour due to cyclic loading.

The model uses 15 input parameters which can be evaluated from standard types of laboratory tests comprising:

(*a*) 1–D compression tests with load reversals and lateral stress measurements
(*b*) resonant column (or similar tests) to estimate the small strain elastic shear modulus
(*c*) undrained triaxial shear tests on K_0-consolidated clay in compression (at OCR's = 1, 2) and extension (at OCR = 1) modes of shearing.

Whittle (1990) describes the selection of input parameters for several types of soil including Boston Blue Clay.

Figures 2 and 3 illustrate the predictive capabilities and limitations of the two models through comparisons with undrained plane strain shear data for K_0-normally consolidated Boston Blue clay measured in the Directional Shear Cell (DSC; Arthur et al., 1977). The DSC device can apply both shear and normal stresses to four faces of a cubical sample and hence control principal stress directions in the plane of loading. Seah (1990) performed a series of tests on K_0-normally consolidated BBC which apply incremental principal stresses oriented at an angle δ_{inc} to the principal consolidation stress direction (σ'_{vc}; Fig. 2). The data for $\delta_{inc} = 0°$ and 90° correspond to plane strain active and passive modes of shearing and match closely data reported previously by Ladd et al.

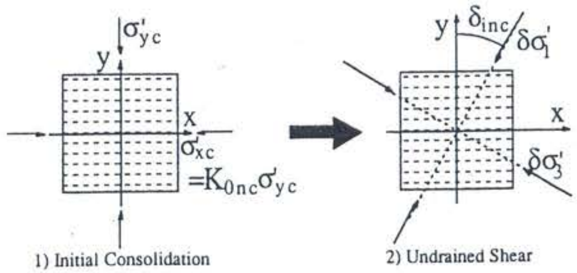

Fig. 2. Test procedure for DSC tests at OCR = 1 (Seah, 1990): (1) initial consolidation, (2) undrained shear

(1971). Tests at intermediate values of δ_{inc} produce continuous rotations of principal stress directions and hence, provide an initial basis for evaluating model predictions of in situ tests with principal stress rotations.

Figures 3(*a*) and (*b*) compare the predicted and measured maximum shear stress–strain response for the MIT-E3 and MCC models (Whittle et al., 1992). The MIT-E3 model describes accurately the undrained shear strengths at $\delta = 0$ and 90° ($s_{uPSA}/\sigma'_{vc} = 0.34$, $s_{uPSP}/\sigma'_{vc} = 0.18$; Fig. 3(*a*) as well as shear strains to peak resistance ($\gamma_p \approx 0.6\%$ and $\gamma_p \geq 6\%$, respectively), and post-peak strain softening in the active shear mode

Table 1. Undrained shear strength ratios for Boston Blue clay at OCR = 1 and 4

OCR	1.0		5.0	
K_0	0.48–0.53		0.75–1.0	
Undrained Strength Ratio	MIT-E3	Measured BBC	MIT-E3	Measured BBC
s_{uTC}/σ'_{vc}	0.33	0.33	1.16	1.04
s_{uTE}/σ'_{vc}	0.15	0.14	0.40	0.52–0.60
s_{uPSA}/σ'_{vc} (1)	0.34	0.34	1.18	0.84–1.04
s_{uPSP}/σ'_{vc} (1)	0.18	0.16–0.19	0.44	0.52–0.60
s_{uDSS}/σ'_{vc} (2)	0.21	0.20	0.72	0.56–0.64
s_{uPM}/σ'_{vc} (3)	0.21	0.21	0.68	0.64–0.76

(1) See Figs. 2, 3.
(2) Direct simple shear, $s_{uDSS}/\sigma'_{vc} = \tau_{hMAX}/\sigma'_{vc}$.
(3) Pressuremeter mode, see Fig. 7.

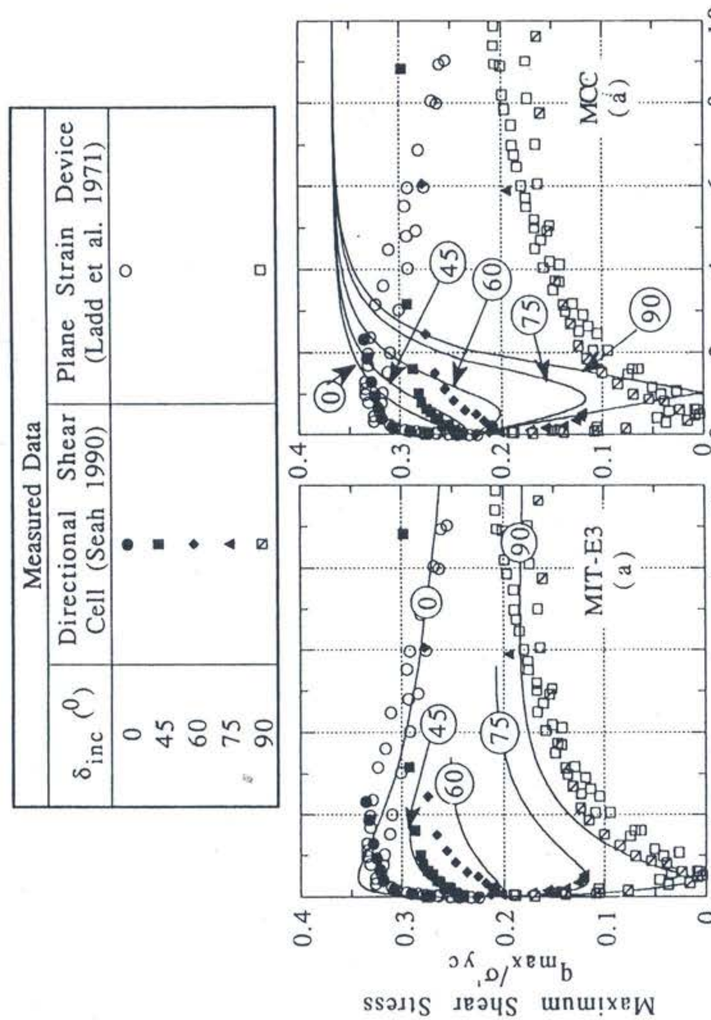

Fig. 3. Evaluation of model predictions for undrained plane strain DSC tests with principal stress rotation

Fig. 4 (below and facing page). Excess pore pressures around the simple pile

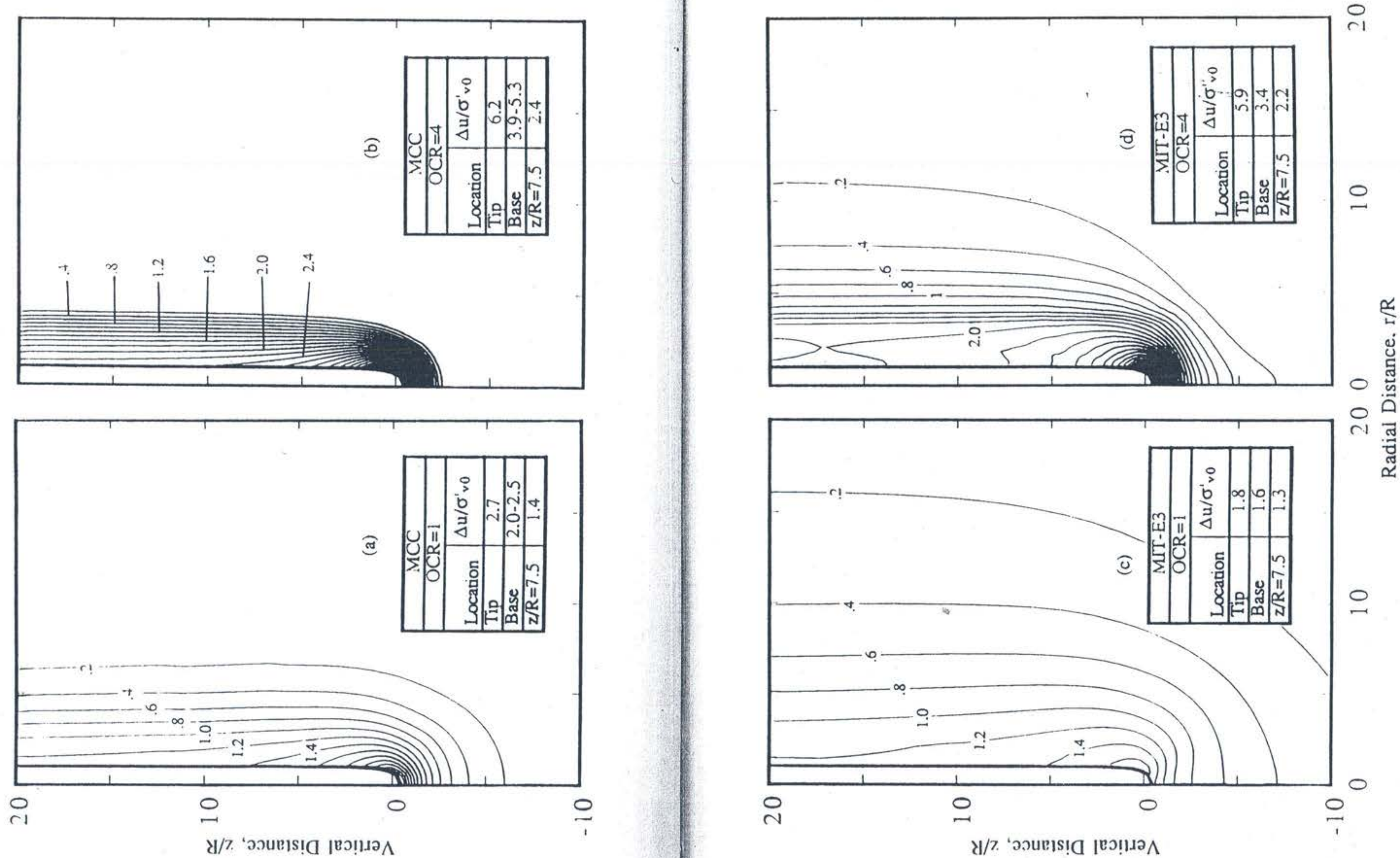

(Fig. 3(*a*))). The model is in good agreement with tests performed at intermediate load directions, $\delta_{inc} = 45$, 60 and 75°.

The MCC model predicts a unique undrained shear strength which is mobilized at large strain, 'critical state' conditions and thus, overestimates significantly the measured shear strength for plane strain shear modes with $\delta > 0°$. The effective stress paths for $\delta_{inc} = 60$, 75 and 90° (Fig. 3(*b*)) show clearly the elastic region of the model, which is not observed in the measured data. Overall, the comparisons show important limitations of simple, isotropic models for describing the anisotropic stress–strain behaviour which is typically measured for K_0-consolidated clays.

Table 1 summarizes MIT-E3 predictions of undrained shear strength ratios measured for Boston Blue clay in a variety of undrained shear modes for tests at OCR = 1.0 and 4.0. This table confirms the model capabilities for describing reliably the 'inelegant plethora' (Wroth, 1984) of undrained shear strengths measured in different modes of shearing.

Piezocone penetration

The simultaneous measurement of cone resistance and pore pressures during steady penetration give the piezocone unique capabilities for estimating soil stratification (e.g. Baligh et al. (1981)). However, the interpretation of engineering properties from these measurements relies primarily on empirical correlations. There are two main factors which limit the quantitative interpretation of piezocone data:

(*a*) There is no simple theory which is capable of describing the complex stress changes induced in the soil during the penetration process. Strain path analyses describe complex interactions of different shear modes, together with reversals in direction, which are not well approximated by simple cavity expansion methods. Similarly, the laboratory element tests demonstrate clearly the differences in the measured stress–strain response in different modes of shearing. This behaviour cannot be explained using simple, isotropic constitutive models.

(*b*) There is a lack of standardization in the design of piezocone equipment and test procedures. Numerous factors can affect significantly the quality of the measured data (e.g. Jamiolkowski et al. (1985)) including

(1) load cell resolution
(2) poor de-airing of filter elements
(3) imprecise calibration of instrumentation.

From an interpretation perspective, there are two design features which are of particular importance:

(*a*) a vertical equilibrium correction factor is usually applied to the measured tip resistance in order to account for pore pressures acting behind the cone

(*b*) there is no standard location for the porous filter element(s), although measurements show that pore pressures vary significantly from the tip of the cone to positions along the shaft (Levadoux and Baligh, 1986).

Figure 4 shows strain path predictions of excess pore pressure ($\Delta u/\sigma'_{v0}$) contours for a simple pile penetrating in Boston Blue clay using the Modified Cam Clay and MIT-E3 models at OCR's = 1 and 4. The results show the following:

(*a*) Undrained piezocone penetration develops large excess pore pressures in normally and lightly overconsolidated BBC. There are large gradients of excess pore pressure, especially at locations around the penetrometer tip and extending vertically to a distance, $z/R \approx 5$. Maximum excess pore pressures occur at or very close to the tip of the penetrometer.

(*b*) MIT-E3 (Figs. 4(*c*), (*d*)) predicts a much larger zone of excess pore pressures around the penetrometer than the MCC model (extending laterally to radial distances, $r/R \approx 30$ and 7, respectively). These distributions of penetration pore pressures are of particular importance for the interpretation of subsequent dissipation measurements.

(*c*) The two soil models predict very similar excess pore pressures acting at the pile shaft ($z/R \geq 10$). This result is surprising in view of the large differences in stress–strain response described in the previous section, and cannot be attributed to any single property of the clay. Large differences in the computed excess pore pressures at the tip of the penetrometer for normally consolidated BBC (MCC predictions are up to 40% higher than MIT-E3) have been explained, in part, by post-peak strain softening modelled by MIT-E3 (Whittle et al., 1991).

(*d*) The magnitudes of excess pore pressures, predicted at all locations around the penetrometer, increases very significantly with OCR (values are shown in Fig. 4). The changes in excess pore pressure are most pronounced at locations close to the tip, while more modest changes occur at locations around the pile shaft. These results indicate that filter locations on the tip or face of the piezocone are more sensitive indicators of variations in undrained shear strength or stress history than those elements located on the shaft.

The strain path predictions for Boston Blue clay can be evaluated through direct comparisons with piezocone measurements. For example, Fig. 5 compares predictions and measurements of net cone resistance, $(q_t - \sigma_{v0})/\sigma'_{v0}$, and excess pore pressures (measured at the

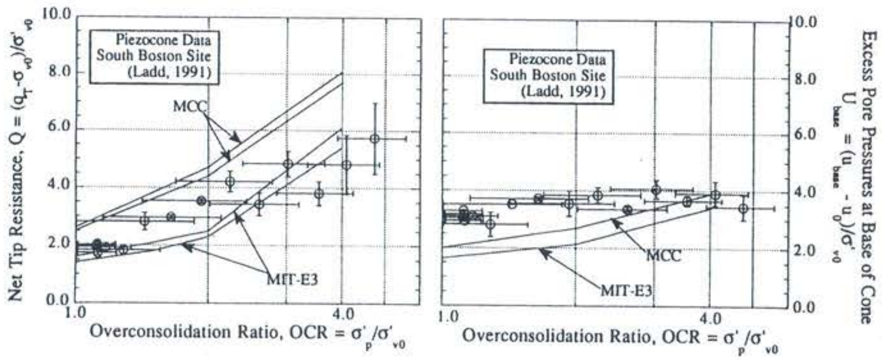

Fig. 5. Comparison of predictions with piezocone measurements in BBC

base of the cone), $(u_2 - u_0)/\sigma'_{v0}$, for a 60 m deep clay layer at a site in South Boston. The stress history (OCR) at this site is well defined from an extensive program of laboratory (incremental oedometer and CRS) consolidation tests (Ladd, 1991). The reported piezocone data represent average values recorded over 1.5 m penetration intervals, while the error bars indicate the extreme measured values and uncertainties in the stress history over this same interval.

The results in Fig. 5 show that MIT-E3 predictions are in good agreement with the measured net tip resistance (Fig. 5(*a*)) and with the base pore pressures measured at OCR$\approx$4 (Fig. 5(*b*)). However, this model underestimates significantly the pore pressures for OCR<4. In comparison, the MCC model overpredicts the measured tip resistance (typically by 30–50%), and gives slightly higher base pore pressures than MIT-E3. The quantitative agreement between tip resistance measurements and MIT-E3 predictions in Fig. 5(*a*) is encouraging. However, the underprediction of penetration pore pressures is consistent with all previous strain path analyses (e.g., Levadoux and Baligh (1980)) and further research is necessary in order to identify factors which contribute to this behaviour.

The numerical predictions provide a basis for evaluating empirical correlations between piezocone penetration measurements and engineering properties of Boston Blue clay. For example, Fig. 6 summarizes the predicted dimensionless measurement ratios $Q = (q_T - \sigma_{v0})/\sigma'_{v0}$, $U_{tip} = (u_1 - u_0)/\sigma'_{v0}$, $U_{base} = (u_2 - u_0)/\sigma'_{v0}$ and $U_{shaft} = (u_3 - u_0)/\sigma'_{v0}$ as functions of the reference undrained shear strength ratio, s_{uTC}/σ'_{v0}, for the MCC and MIT-E3 models at OCRs$\leq$4.

The correlation between net tip resistance, Q and undrained shear strength is almost linear with gradient, N_{KT}, referred to as the 'cone factor'. Existing empirical correlations (e.g. Rad and Lunne (1988)) report

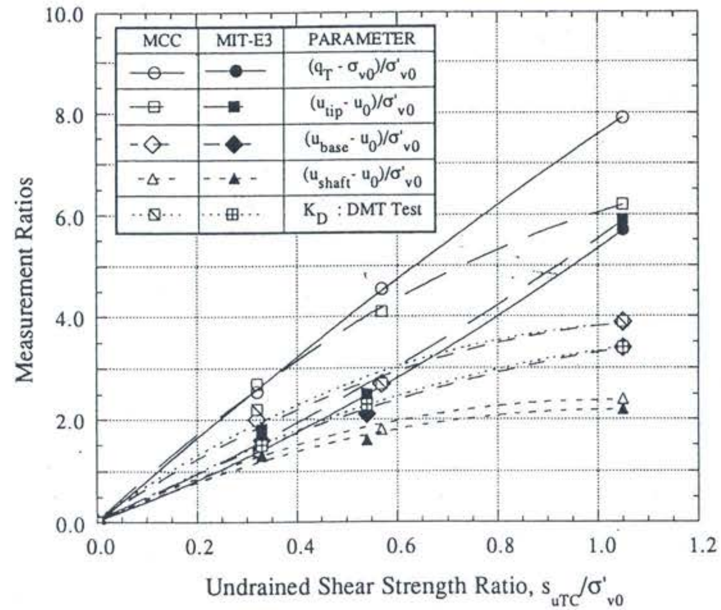

Fig. 6. Evaluation of undrained shear strength from piezocone predictions for Boston Blue clay at OCR$\leq$4

N_{KT} = 5–20 and thus, the predicted cone factors ($N_{KT}\approx$7.5 for MCC; $N_{KT}\approx$5.4 for MIT-E3) are at the low end of the measured range of behaviour. The predictions of tip resistance are controlled primarily by soil properties in the triaxial compression shear mode including

(*a*) the strain to peak shear resistance (yield strain)
(*b*) small strain non-linearity
(*c*) post-peak strain softening.

Although N_{KT} is not a universal constant for all clays, the results in Fig. 6 suggest that cone resistance is the most reliable measurement for estimating changes in undrained strength within a given soil deposit.

Excess pore pressures measured at the tip (or on the face) of the piezocone are also sensitive indicators of undrained shear strength. For the MIT-E3 model, the linear pore pressure factor $N^1_{\Delta u}$ $(=(u_1 - u_0)/s_{uTC})\approx 5.2$, is similar in magnitude to the cone factor. However, the MCC predictions show a non-linear relation between U_{tip} and undrained shear strength. The base and shaft pore pressures are less sensitive to changes in s_{uTC}/σ'_{v0} and hence, are less reliable measurements from which to estimate the undrained shear strength.

Plate penetration

The disturbance caused by undrained penetration affects the interpretation of in situ measurements using plate shaped penetrometers such as the dilatometer, earth pressure cells and the field vane. Whittle et al. (1991) describe comprehensive strain path analyses of these devices using the 'simple plate' geometry (Fig. 1(*b*)). Figure 7 summarizes contours of excess pore pressures, predicted in a horizontal plane far above the penetrating tip, for plates with aspect ratios, B/w = 1, 6.8, 20 and 32.5. The results show the following:

(*a*) The aspect ratio has little influence on the magnitude of excess pore pressure acting at the centre of the plate. However, pressures at

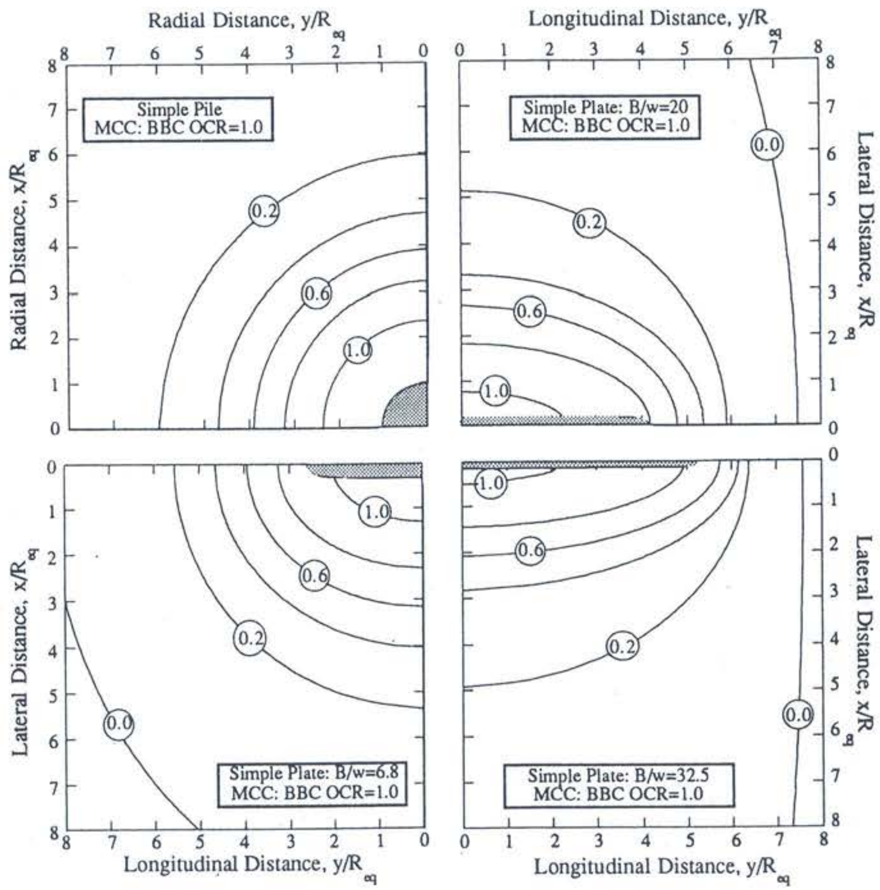

Fig. 7. Excess pore pressures for flat plate penetrometers using the MCC model for normally consolidated BBC

the edge of a slender plate (B/w = 20, 32.5) are typically 20% less than those predicted at the centre. These results are not affected significantly by the soil model or stress history (Whittle et al., 1991).

(*b*) The lateral extent of excess pore pressures is controlled by the equivalent radius, R_{eq}, of the plate. The MCC predictions (Fig. 7) show excess pore pressures extending to lateral distances, $x/R_{eq} \approx 7$–8 for all four plate geometries, while the MIT-E3 model predicts a much larger zone of disturbance (R_{eq} = 20–30, cf. fig. 4).

The lateral effective stress acting on the shaft of an axisymmetric or plate penetrometer during installation differ significantly from the in situ effective stress ratio, K_0. Figure 8 compares K_0 values for Boston Blue clay with strain path predictions of $K_i = \sigma'_{xx}/\sigma'_{v0}$ for different penetrometer geometries, soil models and initial OCRs. For normally and lightly overconsolidated BBC (OCR $\leq$ 4) these solutions show that penetrometer installation reduces significantly the lateral effective stress in the soil. The practical implications of these results are:

(*a*) excess pore pressures are similar in magnitude to the total lateral stress measurements during plate installation

(*b*) it is difficult to make reliable interpretation of K_0 stresses based on installation measurements.

Plate installation stresses and pore pressures have direct application in evaluating dilatometer measurements. The standard dilatometer (Mar-

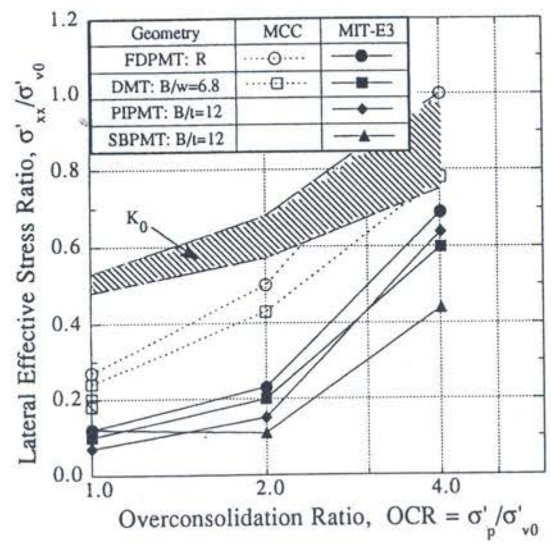

Fig. 8. Lateral effective stresses at penetrometer shaft for Boston Blue clay

chetti, 1980) test procedure measures 'contact pressures', p_0, acting over a centrally located, circular steel diaphragm ($A \approx 28\ cm^2$) immediately after installation. Empirical correlations then relate the dimensionless, horizontal stress index, K_D ($=(p_0 - u_0)/\sigma'_{v0}$) to K_0 and the stress history (OCR) of the soil. Figure 6 shows that strain path predictions of K_D for BBC are practically identical in magnitude to the excess pore pressures measured at the base of the cone. Further studies (Whittle et al., 1991) have found no simple correlations between contact pressures (using dimensionless groups, ($p_0 - \sigma_{h0}/\sigma'_{v0}$ etc.)) and either K_0, stress history or undrained shear strength (assuming normalized soil behaviour).

Undrained shear strength from pressuremeter tests

The interpretation of undrained shear strength from self-boring pressuremeter measurements can be obtained by the theoretical framework of one-dimensional, cylindrical cavity expansion analyses. This section describes simplified strain path analyses which evaluate the effects of installation disturbance on the subsequent interpretation of undrained shear strength for both displacement and self-boring pressuremeters.

The ideal, undrained pressuremeter shear mode can be simulated in a laboratory element test using the True Triaxial device or the Directional Shear Cell. The soil element is initially consolidated under one-dimensional (K_0) conditions (corresponding to the initial stress history in

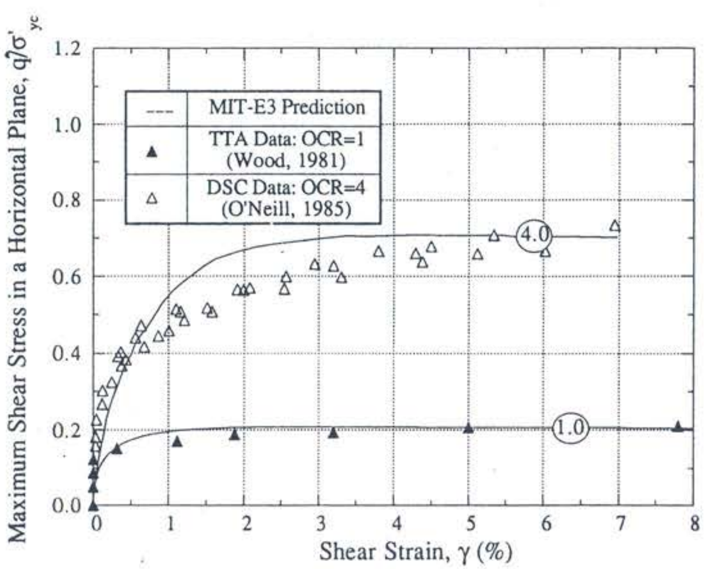

Fig. 9. Comparison of MIT-E3 predictions with measured data for undrained pressuremeter mode of shearing for Boston Blue clay

the ground), and is then sheared, in a plane strain mode at constant volume, in the plane normal to the direction of consolidation. Figure 9 shows the measured shear stress–strain response for pressuremeter element tests on K_0-consolidated Boston Blue Clay at OCR's = 1, 4. The measured data show that the undrained shear strength is mobilized at shear strains of $\gamma \approx 5\%$, and give no indication of post-peak strain softening. Table 1 shows that the undrained shear strength ratios, s_{uPM}/σ'_{v0}, are similar to those measured in the direct simple shear mode. Predictions of the MIT-E3 model (Fig. 9) match closely the measured behaviour (especially the undrained shear strengths) at both OCRs, but tend to overestimate the material stiffness.

In the field situation, pressuremeter installation induces spatial variations in the effective stresses and soil properties prior to membrane expansion. The strain path analyses initially focus on radial disturbance effects, which represent conditions far above the tip (or cutting shoe) of the penetrometer. The calculations compare disturbance effects for the 'full displacement' (FDPMT); push-in (PIPMT; B/t = 10–12) and self-boring pressuremeter (SBPMT) devices. Figure 10 reports predictions of the net applied pressure, $P = (p - u_0)/\sigma'_{v0}$, as a function of the current volumetric strain, $\Delta V/V$ (on a logarithmic scale) for K_0-normally consolidated Boston Blue Clay. In the ideal pressuremeter test, there is no installation disturbance and the initial net pressure is equal to the in situ earth pressure coefficient, K_0 (=0.48). The undrained shear strength

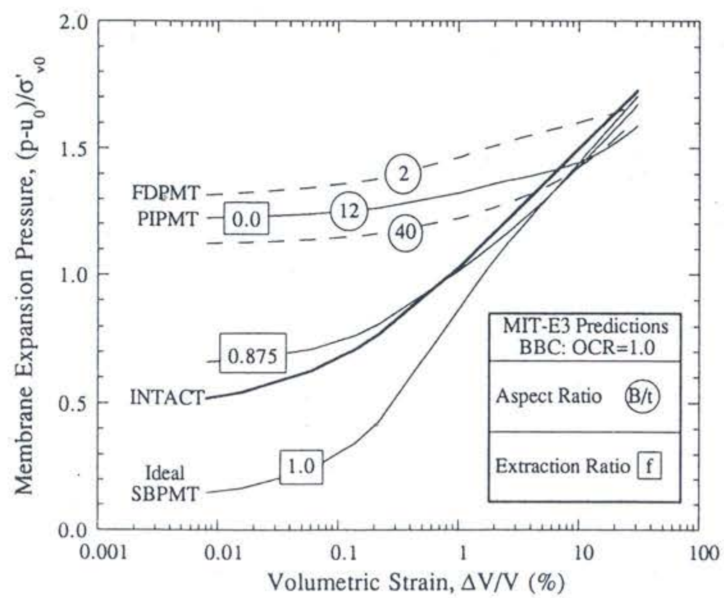

Fig. 10. Predictions of pressuremeter expansion curves for BBC

ratio is computed from the maximum slope of the expansion curve (i.e. $s_u/\sigma'_{v0} = \max\{dP/d\ln \Delta V/V\}$), according to generalized cavity expansion analyses (e.g. Palmer (1972)). For the example shown in Fig. 10, the slope of the undisturbed (intact) expansion curve is approximately linear for $\Delta V/V > 1\%$, and the computed undrained shear strength matches the elemental behaviour described previously.

Installation disturbance caused by full displacement (FDPMT) and push-in pressuremeters (PIPMT) generate large excess pore pressures in the soil (cf. Fig. 4) while reducing the lateral effective stress adjacent to the membrane (Fig. 7). Hence, the net pressure at 'lift-off' (i.e. $\Delta V/V \to 0$) is much larger than the initial K_0 in the soil as shown in Fig. 10. The expansion curves from these displacement pressuremeters are notably more non-linear than the reference undisturbed response. The undrained shear strength is mobilized at large expansion strains and is therefore very difficult to estimate reliably.

The strain path analyses represent steady, self-boring penetration in terms of the volume balance between soil displaced by the pressuremeter and that extracted by the cutting process. Figure 10 shows the pressuremeter expansion curve for an ideal self-boring pressuremeter test (with extraction ratio, f = 1). In this case, excess pore pressures are negligible (lateral effective stresses are shown in Fig. 8) and hence, the

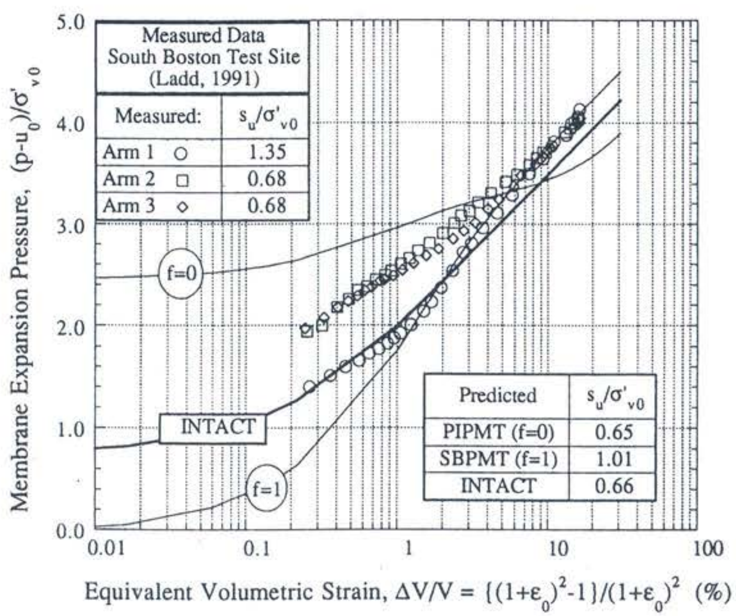

Fig. 11. Evaluation of predicted and measured pressuremeter expansion curves for Boston Blue clay at OCR = 4

lift-off pressure is much smaller than the in situ K_0 condition. Visual inspection of the expansion curve shows that the peak shear resistance occurs at $\Delta V/V \approx 1\%$, while the subsequent curvature implies an apparent post-peak softening.

It is difficult to equate the idealized simulation of self-boring with the parameters which control the cutting process in a real test. As a result, it is not possible to make a true 'prediction' of the field measurements. Figure 11 compares the measured data from a self-boring pressuremeter test in Boston Blue clay at OCR = 4 with the predicted expansion behaviour for three cases:

(1) no disturbance (intact)
(2) push-in penetration (f = 0, B/t = 12)
(3) an ideal SBPMT (f = 1).

The equivalent volumetric strain is computed from the circumferential strains (ε_0) measured by three feeler arms. Although there are significant initial differences in the measured expansion curves, the data coalesce for volumetric strains $\Delta V/V \geq 5\%$, and coincide with the predicted expansion curve for the ideal SBPM test. The apparent shear resistance computed from these curves at large strains (i.e. for all three arms and f = 1) are in good agreement with the reference, undisturbed pressuremeter strength. The measurements for arm 1 coincide with idealized SBPM curve for $\Delta V/V > 1.5\%$ with an interpreted peak shear strength approximately 50–100% higher than that of the intact clay. Differences in the simulated and measured expansion curves at small strain levels may indicate the importance of factors not considered in the analysis such as internal pressures inside the cutting shoe, or soil consolidation prior to membrane expansion (the test in Fig. 11 was performed after a 30 min 'relaxation period').

Figure 12 summarizes the predictions of undrained shear strength for normally consolidated Boston Blue clay from the pressuremeter expansion curves as functions of:

(*a*) the aspect ratio, B/t, for displacement penetration
(*b*) the extraction ratio, f, for self-boring penetration.

The error bars correspond to tests in which the peak shear resistance develops at large volumetric strains. Undrained shear strengths from displacement pressuremeter (FDPM, PIPM) expansion curves underestimate significantly the true pressuremeter shear strength ($s_{uPM}/\sigma'_{vc} = 0.21$). In contrast, the predictions for self-boring tests with extraction ratios, $0.85 \leq f \leq 1$, estimate peak shear strengths up to 50% higher than the true behaviour. The interpreted shear strengths agree qualitatively with measurements from different types of pressuremeter reported by Lacasse et al. (1990). Further studies are now required to

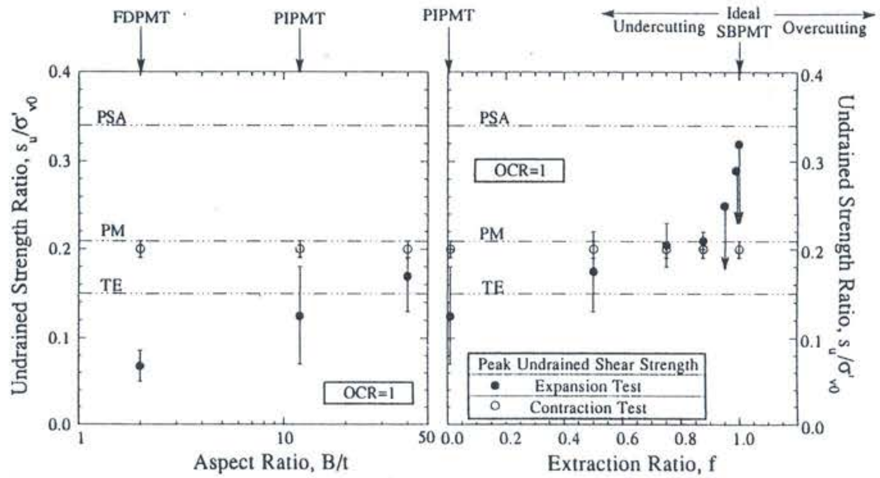

Fig. 12. Summary of interpreted undrained shear strengths from pressuremeter predictions for Boston Blue clay

establish the effects of installation disturbance for the overcutting mode of penetration ($f > 1$), and to refine the analyses through the inclusion of finite membrane length, proximity to the cutting shoe, etc.

Figure 12 also shows undrained shear strengths interpreted from predictions of the pressuremeter contraction response, as originally proposed by Houlsby and Withers (1988) for the full displacement pressuremeter (FDPMT). The predictions show that:

(*a*) there is much less ambiguity in the interpretation of undrained shear strength from the contraction curve

(*b*) the interpreted undrained shear strength ratio is in excellent agreement with s_{uPM}/σ'_{vc} (measured in laboratory tests), and is not affected by the installation disturbance (for the range of conditions considered in this paper).

These results suggest that undrained shear strength can be reliably estimated from the contraction curve. Further evaluations of this method are currently in progress.

Conclusions

This paper has presented a systematic analysis of the effects of installation disturbance on in situ measurements in clay. The analyses apply the strain path method, together with generalized effective stress soil models (MCC and MIT-E3), in order to predict in situ measurements for tests performed in Boston Blue clay (BBC). Detailed evaluations of

the constitutive models demonstrate that MIT-E3 provides reliable predictions of the anisotropic, stress-strain behaviour measured in laboratory tests on K_0-consolidated BBC with $1 \leq \text{OCR} \leq 4$.

The strain path predictions are in good agreement with measurements of cone resistance obtained from piezocone tests at a site in South Boston, but generally underpredict the penetration pore pressures at the base of the cone. The numerical predictions also show that the net tip resistance ($q_T - \sigma_{v0}$) responds almost linearly to cones in the undrained shear strength for a given soil model (i.e. this implies N_{KT} is a constant for a given soil type). Excess pore pressures measured at the tip (or on the face of) the piezocone are also well correlated through the factor $N_{\Delta u}$; while measurements at the base of the cone, or at locations along the shaft, are significantly less responsive to changes in the shear strength.

The strain path analyses show that there are strong similarities in the stresses and pore pressures predicted around flat plate and axisymmetric penetrometers. The plate aspect ratio, B/w, controls the distribution of stresses around the penetrometer, while the equivalent radius, R_{eq}, controls the lateral extent of the disturbance. Predictions of contact pressures, measured immediately after installation by the Marchetti dilatometer, are similar in magnitude to the excess pore pressures measured at the base of a piezocone.

The analyses show that installation procedures affect the interpretation of undrained shear strength from pressuremeter expansion tests. For displacement pressuremeter tests in K_0-normally consolidated BBC, the interpreted undrained shear strength ratio, $s_u/\sigma'_{vc} \approx 0.07$–$0.12$, is significantly lower than the true material response ($s_{uPM}/\sigma'_{vc} = 0.21$). In contrast, simplified simulations of self-boring show interpreted strength ratios up to $s_u/\sigma'_{vc} = 0.32$ for 'idealized' SBPM tests. Further analyses show that interpretation methods using pressuremeter contraction measurements give $s_u/\sigma'_{vc} = 0.20$ and are insensitive to the effects of installation disturbance.

Acknowledgements

This work was supported by the Air Force Office of Scientific Research through grant AFOSR-89-0060. The authors are grateful to Professor Charles Ladd for his assistance in the interpretation of the field data from the South Boston test site. These data were obtained by Haley and Aldrich, Inc. as part of the Central Artery/Third Harbour Tunnel project in Boston.

References

Arthur, J.R.F., Chua, K.S. and Dunstan, T. (1977). Induced anisotropy in a sand. Géotechnique, Vol. 27, No. 1, pp. 13–36.

AUBENY, C.P. (1992). Rational interpretation of in-situ tests in cohesive soils. PhD Thesis. MIT, Cambridge, MA.

BALIGH, M.M. (1985). Strain Path Method. ASCE Journal of Geotechnical Engineering, Vol. 111, No. GT9, pp. 1108–1136.

BALIGH, M.M. (1986a). Undrained deep penetration: I. Shear stresses. Géotechnique, Vol. 36, No. 4, pp. 471–485.

BALIGH, M.M. (1986b). Undrained deep penetration: II. Pore pressures. Géotechnique, Vol. 36, No. 4, pp. 487–501.

BALIGH, M.M., AZZOUZ, A.S., WISSA, A.E.Z., MARTIN, R.T. AND MORRISON, M.J. (1981). The piezocone penetrometer. Proceedings ASCE Symposium on Cone Penetration Testing and Experience, St Louis, MO., pp. 247–263.

BALIGH, M.M., AZZOUZ, A.S. AND CHIN, C.T. (1987). Disturbances due to 'ideal' tube sampling. ASCE Journal of Geotechnical Engineering, Vol. 113, No. GT7, pp. 739–757.

ELGHAIB, M.K. (1989). Prediction and interpretation of piezocone tests in clays, sands and silts. PhD Thesis, MIT, Cambridge, MA.

HOULSBY, G.T. AND WITHERS, N.J. (1988). Analysis of cone pressuremeter test in clay. Géotechnique, Vol. 38, No. 4, pp. 575–589.

JAMIOLKOWSKI, M., LADD, C.C., GERMAINE, J.T. AND LANCELLOTTA, R. (1985). New developments in field and laboratory testing of soils. Proceedings 11th Intl. Conf. on Soil Mechs. and Foundation Engrg., San Francisco, CA. Vol. 1, pp. 57–153.

LACASSE, S.L., D'ORAZIO, T.D. AND BANDIS, T.B. (1990). Interpretation of self-boring and push-in pressuremeter tests. Pressuremeters, ICE, London, pp. 273–285.

LADD, C.C., BOVEE, R., EDGERS, L. AND RIXNER, J.J. (1971). Consolidated undrained plane strain tests on Boston Blue Clay. MIT Research Report R71–13.

LADD, C.C. (1991). Personal communication.

LEVADOUX, J.-N. AND BALIGH, M.M. (1980). Pore pressures in clays due to cone penetration. MIT Research Report R80–15.

LEVADOUX, J.-N. AND BALIGH, M.M. (1986). Consolidation after undrained piezocone penetration. I: Prediction. ASCE Journal of Geotechnical Engineering, Vol. 112, No. GT7, pp. 707–726.

MARCHETTI, S. (1980). In-situ tests by flat dilatometer, ASCE Journal of Geotechnical Engineering, Vol. 106, No. GT3, pp. 299–321.

O'NEILL, D.A. (1985). Undrained strength anisotropy of an overconsolidated, thixotropic clay. SM Thesis. MIT, Cambridge, MA.

PALMER, A.C. (1972). Undrained plane strain expansion of a cylindrical cavity in clay: a simple interpretation of the pressuremeter test. Géotechnique, Vol. 22, No. 3, pp. 451–457.

RAD, N.S. AND LUNNE, T. (1988). Direct correlations between piezocone

test results and undrained shear strength of clay. Proceedings ISOPT 1, Orlando, FL, Vol. 2, pp. 911–918.

ROSCOE, K.H. AND BURLAND, J.B. (1968). On the generalized stress–strain behaviour of 'Wet' clay. Engineering Plasticity, Eds. J. Heyman and F.A. Leckie, Cambridge University Press, pp. 535–609.

SEAH, T.H. (1990). Anisotropy of resedimented Boston Blue Clay. PhD Thesis, MIT, Cambridge, MA.

TEH, C.-I. AND HOULSBY, G.T. (1991). An analytical study of the cone penetration test in clay. Géotechnique, 41, No. 1, pp. 1–17.

WHITTLE, A.J. (1990). A constitutive model for overconsolidated clays. MIT Sea Grant Report, MITSG 90–15.

WHITTLE, A.J. (1992). Evaluation of a constitutive model for overconsolidated clays. Géotechnique, 1993, Vol. 43.

WHITTLE, A.J., AUBENY, C.P., RAFALOVICH, A., LADD, C.C. AND BALIGH, M.M. (1991). Prediction and interpretation of in-situ penetration tests in cohesive soils. MIT Research Report, R91–01.

WHITTLE, A.J., DEGROOT, D.J., SEAH, T.H. AND LADD, C.C. (1992). Evaluation of model predictions of the anistropic behaviour of Boston Blue Clay. Submitted to ASCE Journal of Geotechnical Engineering.

WOOD, D.M. (1981). True triaxial tests on Boston Blue Clay. Proceedings 10th Intl. Conf. on Soil Mechs. and Foundation Engrg., Stockholm, pp. 825–830.

WROTH, C.P. (1984). The interpretation of in-situ soil tests, Géotechnique, 34, No. 4, pp. 449–489.

WROTH, C.P. AND HUGHES, J.M.O. (1973). An instrument for the in-situ measurement of the properties of soft clays. Proceedings 8th Intl. Conf. on Soil Mechs. and Foundation Engrg., Moscow, Vol. 1.2, pp. 487–494.